

From exhaustive simulations to key principles in DNA nanoelectronics

Roman Korol and Dvira Segal

*Department of Chemistry and Centre for Quantum Information and Quantum Control,
University of Toronto, 80 Saint George St., Toronto, Ontario, Canada M5S 3H6*

(Dated: December 25, 2017)

Charge transfer can take place along double helical DNA over distances as long as 30 nanometers. However, given the active role of the thermal environment surrounding charge carriers in DNA, physical mechanisms driving the transfer process are highly debated. Moreover, the overall potential of DNA to act as a conducting material in nanoelectronic circuits is questionable. Here, we identify key principles in DNA nanoelectronics by performing an exhaustive computational study. The electronic structure of double-stranded DNA is described with a coarse-grained model. The dynamics of the molecular system and its environment is taken into account using a quantum scattering method, mimicking incoherent, elastic and inelastic effects. By analyzing all possible sequences with 3 to 7 base pairs, we identify fundamental principles in DNA nanoelectronics: The environment crucially influences the electrical conductance of DNA, and the majority of sequences conduct via a mixed, coherent-incoherent mechanism. Likewise, the metal-molecule coupling and the gateway states play significant roles in the transport behavior. While most sequences analyzed here are exposed to be rather poor electrical conductors, we identify exceptional DNA molecules, which we predict to be excellent and robust conductors of electric current over a wide range of physical conditions.

I. INTRODUCTION

Is DNA a good conductor of electricity? Experiments evince that a double-helix DNA can support long range charge transfer along its axis given the good overlap of π orbitals of neighboring bases. Charge transport processes in DNA are central to applications in biology, chemistry, physics, and engineering [1]. Charge transfer plays a crucial role in damage and repair processes in DNA, thus in the development of cancer in the living cell [2, 3]. Moreover, DNA is an attractive material for nanoscale engineering and electronic applications: With its recognition abilities, self-assembly, controllability, structural flexibility, and rich electronic properties, it can serve either as the template for nanostructures of desired shapes and function, or as the conducting compound in molecular electronic circuits [4–7].

Experiments demonstrate highly diverse charge transport behavior through DNA. In ultra long molecules with hundreds of base-pairs (bp), the measured resistance covers the full range of values characteristics to metals, semi-conductors, and insulating materials [8]. Nanoscale (5-20 bp) DNA duplexes are agreed to be conducting, yet measurements demonstrate a broad range of trends [8]. This vast variation is not surprising. Charge transfer within a complex molecule such as DNA is influenced by multiple factors. Depending on the molecular content and the base sequence [9–12], length [9, 13–16], backbone composition [17], environmental conditions [18], temperature, helical conformation [19], linkers to the electrodes [17, 20, 21] and voltage-gating [22], the four bases of DNA can form sequences that act, for example, as tunnelling barriers [9, 16], ohmic resistors [9, 15, 16], resonant-ballistic or intermediate coherent-incoherent conductors [23–26]. It is apparent that exploring charge transport characteristics within a *singular* DNA sequence cannot contribute general insights as to the potential of the double helix DNA to serve as an electronic material.

Given this diversity, what valuable information can computational science contribute to DNA electronics? Rather than focusing on a particular sequence, we search here for fundamental trends and assess the capacity of DNA to conduct electric current under different conditions. The elementary components of DNA are four nucleotides forming double stranded helix DNA (dsDNA). The strands are hybridized by obeying the base-pairing rules, adenine (A) with thymine (T) and cytosine (C) with guanine (G). Sequences with 3 – 8 base pairs are 10-30 Å long, an extended distance for charge transfer in condensed phases. By studying the electrical conductance of all such DNA sequences, we henceforth ask the following questions: (i) What is the distribution of conduction values for these junctions? Are most combinations good or poor conductors? (ii) What are the physical mechanisms driving charge transfer under different environmental conditions? (iii) How susceptible is DNA conductance to temperature, structural and environmental fluctuations, or the contact to the metals? (iv) Which sequences are excellent conductors—and relatively insensitive to environmental interactions?

We address these questions with a brute force method, by performing exhaustive numerical simulations. For a given length (number of base-pairs) n , we consider all possible sequences satisfying the base-pairing rules, and simulate the electrical conductance of these compounds in the geometry of a metal-molecule-metal junction. Such an ambitious mission can only be accomplished by using a reasonable, economical method. We employ a tight-binding ladder model

to represent the electronic structure of the double helix. To take into account the impact of structural dynamics (intra and inter-molecular motion), we perform transport simulations using the Landauer-Büttiker’s probe (LBP) method [27, 28]. In this approach, the interaction of charge carriers with atomic motion is included in a phenomenological manner by introducing a tunable parameter, which is responsible for decoherence and energy exchange processes. The LBP method covers different transport mechanisms, from pure coherent conduction with frozen nuclei to the ohmic limit, when electronic coherence is fully lost and diffusive motion prevails [19, 29–42]. As well, the LBP method can meaningfully capture intermediate coherent-incoherent transport behavior [43].

Previous studies were performed on particularly designed, interesting strands, often revealing signatures of three limiting mechanisms: (i) quantum coherent “superexchange” transmission through an A:T block, serving as a tunneling barrier, (ii) coherent band-like “molecular wire” conduction, with charge delocalizing along e.g. stacked G:C sequences, and (iii) sequential multi-site incoherent hopping. In the latter case, environmental degrees of freedom such as intramolecular vibrations localize conducting charges on each G site. This multi-step hopping process is characterized by an ohmic behavior, a linear enhancement of the electronic resistance with molecular length. A principal finding of our analysis is that the classification of transport mechanisms as coherent tunnelling, coherent-ballistic, or thermalized multi-site hopping is appropriate for very few strands. The majority of the examined DNA junctions, operating in ambient conditions, follow an intermediate, quantum coherent-incoherent mechanism. Quantum coherent effects are therefore prevalent and influential in biological electron transport over distances as long as 40 Å.

II. MODEL AND METHOD

A. Setup

We model recent conductance measurements of relatively short (8-20 bp) B-form DNA junctions [9, 10, 16, 22, 25, 26]. This type of experiments are conducted using a scanning tunneling microscope (STM) break-junction approach, performed in aqueous solution or in humidified atmosphere at room temperature. In a typical experiment, both the STM tip and the substrate are made of gold, but the tip is further coated with a wax layer to minimize ionic conduction between the electrodes. To ensure strong, chemical binding of the molecule to the electrodes, each DNA molecule is modified with thiol or amine linkers. The substrate is immersed into a buffer solution containing dsDNA. It is then dried with a nitrogen gas, with measurements performed in a humidified atmosphere. STM break-junction measurements are performed thousands of time by repeatedly bringing the tip into and out of contact with the substrate—which is covered with dsDNA molecules within a water layer. The electrical conductance of the junction created in the pulling processes is recorded as a function of the tip-substrate distance; a plateau in the retracting curve indicates on the formation of a molecular junction. Conductance histograms provide the most probable conductance value, as well as estimates over the number of molecules forming the junction and the heterogeneity of the contact geometry.

B. Electronic Hamiltonian

For a given number of base pairs, we draw all possible DNA duplexes; there are 4^n such molecules composed from the four nucleotide bases. Molecules are connected to the metals through the 3’ ends, see Figure 1, mimicking experiments. We model the electronic properties of B-form DNA using a coarse-grained tight-binding ladder Hamiltonian, see e.g. Refs. [44–50]. There is an extensive evidence that holes, rather than electrons, dominate charge migration in DNA, and that charge transport takes place inside the double helix along the π stacking, rather than through the sugar-phosphate skeleton [51–53]. The electronic Hamiltonian describing hole migration in a dsDNA junction reads $\hat{H} = \hat{H}_M + \hat{H}_L + \hat{H}_R + \hat{V}_L + \hat{V}_R$. The molecular term is

$$\hat{H}_M = \sum_{j=1}^n \left[\sum_{s=1,2} \epsilon_{j,s} \hat{c}_{j,s}^\dagger \hat{c}_{j,s} + \sum_{s \neq s'=1,2} t_{j,ss'} \hat{c}_{j,s}^\dagger \hat{c}_{j,s'} \right. \\ \left. + \sum_{s,s'=1,2} t_{j,j+1,ss'} (\hat{c}_{j,s}^\dagger \hat{c}_{j+1,s'} + h.c.) \right]. \quad (1)$$

Each site represents a particular base, $N = 2n$ is the total number of bases. The index $s = 1, 2$ identifies the strand. $\hat{c}_{j,s}^\dagger$ creates a hole on strand s at site J with an on-site energy $\epsilon_{j,s}$. $t_{j,ss'}$ and $t_{j,j+1,ss'}$ are the electronic coupling elements between nearest neighboring bases. The model mimics the topology of dsDNA molecules; helical effects are

taken into account within renormalized electronic parameters. The electrodes (L,R) are modeled as Fermi seas of noninteracting electrons with k as the index for momentum, (fermionic creation operators $\hat{a}_{k,L/R}^\dagger$),

$$\hat{H}_L = \sum_k \epsilon_{k,L} \hat{a}_{k,L}^\dagger \hat{a}_{k,L}, \quad \hat{H}_R = \sum_k \epsilon_{k,R} \hat{a}_{k,R}^\dagger \hat{a}_{k,R}. \quad (2)$$

The first (last) site on the $s = 1$ ($s = 2$) strand is coupled to the left (right) metal lead,

$$\hat{V}_L = \sum_k g_{k,L} \hat{a}_{k,L}^\dagger \hat{c}_{j=1,s=1} + h.c., \quad \hat{V}_R = \sum_k g_{k,R} \hat{a}_{k,R}^\dagger \hat{c}_{j=n,s=2} + h.c. \quad (3)$$

We adapt a DFT- based parametrization; electronic site energies and matrix elements, $t_{j,ss'}$ and $t_{j,j+1,ss'}$, are listed in Ref. [49]. To introduce relevant energy scales, in Table I we list site energies, reported relative to the guanine base, and inter-strand coupling [54].

ϵ_G	ϵ_A	ϵ_C	ϵ_T	$t_{G:C}$	$t_{A:T}$
0	0.453	1.544	1.286	-0.055	-0.047

TABLE I: On-site energies, relative to the guanine base, and inter-strand electronic coupling $t_{j,s \neq s'}$ (eV). The full parameter set for the Hamiltonian (1) is included in Ref. [49].

C. Nuclear Environment

Charge transport through DNA is critically influenced by the surrounding thermal environment, comprising nuclear dynamics of the nucleobase, structural motion, reorganization of solvent molecules around the transferred charge, polarization effects through the backbone and counterions. This fluctuating and correlated environment can be captured, for example, with a coarse-graining approach, by building the effect of the environment on the electronic Hamiltonian within spatially and temporally corrected noise terms [55, 56]. Other approaches are based on combining classical molecular dynamics (MD) simulations with quantum mechanics/molecular mechanics (QM/MM) methodologies [57–62]. One may also explicitly consider the interaction of transport charges with selected internal vibrational modes using the Green’s function formalism [44], quantum rate equations [63], or semiclassical approximations [64].

Here, we use an alternative, low-cost technique and account for system-environment interactions by employing the Landauer-Büttiker probe method [27, 28]. It is applicable for the study of charge conduction in a wide range of systems, from single-atom point contacts up to the thermodynamic limit [19, 29–43, 65]. In this technique, incoherent elastic and inelastic electron (or hole) scattering effects are taken into account by augmenting the non-interacting electronic Hamiltonian with probe terminals through which charge carriers loose their phase memory and possibly exchange energy with other degrees of freedom. The technique was originally introduced to study decoherence effects in mesoscopic devices, yet it was successfully applied to explore electronic conduction in organic and biomolecular systems [19, 32, 33, 35, 36].

We had recently demonstrated that the LBP method can capture different, limiting transport regimes in molecular transport junctions: tunneling conduction, ballistic motion, and incoherent hopping [37]. Moreover, the method can reproduce an intermediate quantum coherent-incoherent transport behavior in a qualitative agreement with experiments on DNA junctions [43]. As described in e.g. Refs. [39, 66], the LBP method can be applied in different fashions so as to control scattering events. Here, we use the so-called “voltage probe” method at low bias, which implements elastic and inelastic scattering processes under low applied bias—within linear response.

The methodology was detailed elsewhere [37–41, 43] and the program was published in [42]. Here, we recount only the essential principles so as to introduce working parameters. We voltage bias the electrodes, $\Delta\mu = \mu_L - \mu_R = eV$ and fix the temperature of the metals at T_{el} . Each electronic site (base), is connected to a “probe”, emulating the dynamical environment, with the hybridization energy γ_d . Charges are allowed to leave the molecule towards the probes, where they loose phase information and absorb or release energy. Nevertheless, we set the chemical potentials of the probes such that the current in the physical system is conserved. The electrical conductance of the junction, in units of $G_0 = e^2/h$, with the electron charge e and Planck’s constant h , is given by

$$G = \frac{1}{V} \sum_\alpha (\mu_L - \mu_\alpha) \int_{-\infty}^{\infty} \mathcal{T}_{L,\alpha}(\epsilon) \left(-\frac{\partial f_{eq}}{\partial \epsilon} \right) d\epsilon. \quad (4)$$

The summation over α includes the physical, source and drain electrodes as well as the probes. Here, $f_{eq}(\epsilon) = [e^{\beta_{el}(\epsilon - \epsilon_F)} + 1]^{-1}$ is the equilibrium Fermi-Dirac distribution function, given in terms of the temperatures $k_B T_{el} = \beta_{el}^{-1}$

and the Fermi energy ϵ_F . The transmission function in Eqs. (4), $\mathcal{T}_{\alpha,\alpha'}(\epsilon) = \text{Tr}[\hat{\Gamma}_{\alpha'}(\epsilon)\hat{G}_T(\epsilon)\hat{\Gamma}_{\alpha}(\epsilon)\hat{G}_a(\epsilon)]$, is expressed in terms of the Green's function, $G_r(\epsilon) = 1/(\epsilon\hat{I} - \hat{H}_M - \hat{\Sigma})$; $\hat{G}_a(\epsilon) = G_r^\dagger(\epsilon)$, and \hat{I} as the identity matrix. The self energy $\hat{\Sigma}$ includes contributions from the electrodes, with the hybridization matrices $\hat{\Gamma}_{\alpha}(\epsilon) = 2\text{Im}\hat{\Sigma}_{\alpha}(\epsilon)$ [67, 68]. Assuming energy independent functions and local couplings, these matrices include a single nonzero element [69]. The metal-molecules hybridization energy is given by $\gamma_{L,R}$. Environmental effects are captured by the parameter γ_d , with \hbar/γ_d as the characteristic elastic and inelastic scattering time of charge carriers. Lastly, to evaluate Eq. (4), the chemical potentials of the probe terminals are determined from an algebraic charge-conservation equation [37–40]. One should note that the probes not only introduce level broadening, but further open up additional, incoherent transfer pathways, as indicated by the appearance of new transmission functions in Eq. (4), beyond the direct L to R contribution.

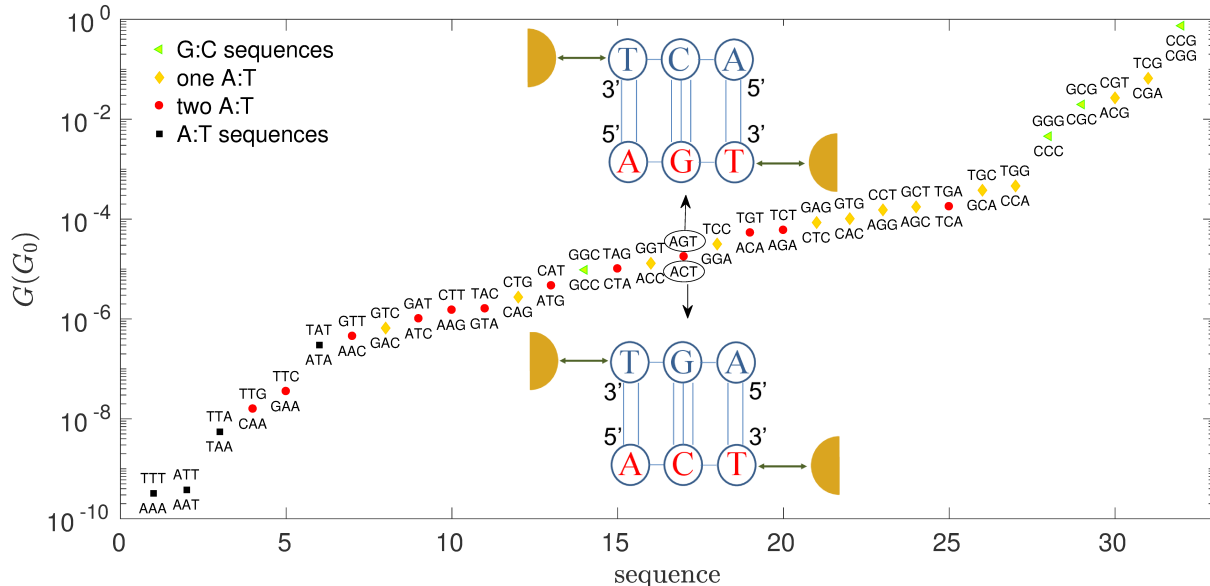


FIG. 1: Electrical conductances of all 32 combinations of 3 bp DNA junctions, $\gamma_d = 0$, $\gamma_{L,R} = 50$ meV, $T_{el} = 5$ K. By convention, sequences are labeled from the 5' to the 3' end. We further sketch the geometry of examined junctions, with the DNA molecule connected to the metals (semi-spheres) at its 3' ends. We assume that the metal contacts are identical, thus, given symmetry, the two sequences displayed show an indistinguishable conductance.

III. RESULTS AND DISCUSSION

A. Choice of parameters

Our model comprises a parameterized electronic tight-binding Hamiltonian for the DNA duplex and additional parameters, γ_d , capturing scattering effects of carriers due to molecular dynamics, and ϵ_F , T_{el} and $\gamma_{L,R}$, describing the electrodes and the metal-molecule hybridization. We now explain our choice of simulated values. The probes emulate decoherence and energy exchange processes at a rate γ_d/\hbar . For DNA in aqueous or humidified conditions at room temperature, previous simulations suggested $\gamma_d = 5 - 30$ meV [19, 34, 40, 41, 43]. We further justify this range as follows. First, calculations corresponding to dry DNA yield $\gamma_d = 1-6$ meV [34], but charge transfer within a wet medium is expected to suffer from stronger environmental effects. Moreover, molecular dynamics simulations of DNA in solution suggest that fluctuations of site energies have a lifetime $\tau \sim 200$ fs [56, 70], which converts to $\hbar/\tau = 20$ meV, within the range of our estimated decay constant.

We perform simulations at $\gamma_d = 0$, corresponding to charge transfer in rigid-frozen structures, and at $\gamma_d = 10$ and 30 meV, representing dsDNA in solution at ambient conditions. We further run simulations at lower (1 meV) and higher (50 meV) values, and confirm that observed phenomena are regularly-monotonously modified by this parameter. Note that electronic tunneling energies in DNA are order of 1-75 meV [49]. We do not explicitly introduce a temperature for the nuclear (molecular, solvent) degrees of freedom, as this temperature is encoded in the magnitude of γ_d . Temperature, denoted by T_{el} , explicitly appears in Eq. (4) and it dictates electronic population in the metals,

thus the broadening of the Fermi function. At high electronic temperature, carriers fill the tail of the Fermi function, which is in resonance with molecular orbitals. This contribution is reflected by an enhanced resonant-ballistic current. In real systems, this delicate, resonant contribution is quickly suppressed by temporal fluctuations of the structure [55]. To capture this suppression effect and reduce the impact of the resonant-band like current, we further test our simulations at a rather low electronic temperature, $T_{el} = 5$ K, bounding injected electrons to the vicinity of the Fermi energy.

We employ two representative values for the metal-molecule coupling, $\gamma_{L,R}=50, 1000$ meV, corresponding to moderate and strong metal-molecule hybridization. Another tunable parameter is the position of the Fermi energy of the metals relative to molecular states. Since the HOMO level of DNA appears close to the Fermi level of gold, compared to its LUMO level, holes (rather than electrons) are the main charge carriers in DNA [14]. The measurement of a positive Seebeck coefficient [16] further affirms this conclusion. Specifically, since the HOMO of the guanine nucleotide lies close to the Fermi energy of the gold electrode, we place ϵ_F on resonance with the on-site energy of the guanine base [19, 34, 40, 41, 43, 45].

We demonstrate below the behavior of $n = 3 - 7$ long sequences, but we had further looked at all combinations with $n = 8$ base pairs. Our observations are retained throughout. Given the strong signatures of observed effects, we expect our conclusions to certainly hold for molecules with $n = 10$ base pair.

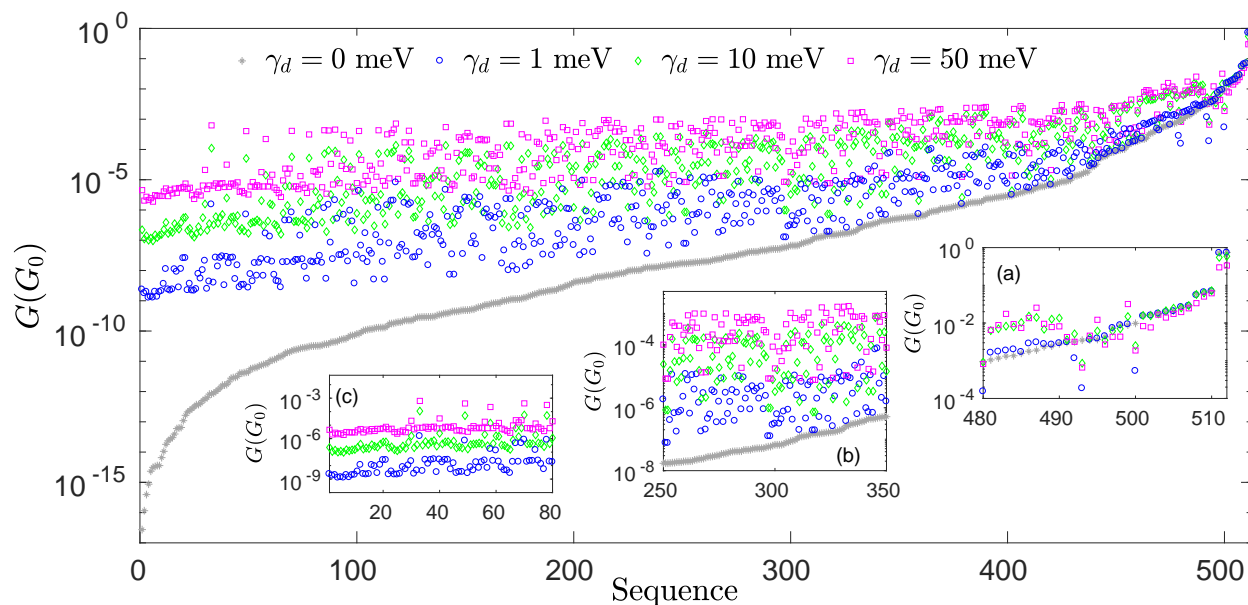


FIG. 2: Conductances of dsDNA with 5 base pairs under increasing environmental effects, $\gamma_d = 0, 1, 10$ and 50 meV. Other parameters are $\gamma_{L,R} = 50$ meV and $T_{el} = 5$ K.

B. Characteristic trends

To illustrate our results, Figure 1 presents the conductance of short ($n = 3$), rigid junctions. Molecules are connected to the electrodes at the 3' terminal, and sequences are labeled by convention 5' to 3'. Every point in this graph corresponds to two sequences, which due to symmetry yield identical values. For an odd number n , there are $4^n/2$ different sequences. For an even n , there are $4^{n/2}$ palindrome sequences such as 5'AATT3', which do not have a twin. Therefore, for $n=4$ we identify $(4^n - 4^{n/2})/2 + 4^{n/2} = 136$ distinct junctions. Counting in this manner, there are 32, 136, 512, 2080, 8192, and 32,896 distinct junctions for $n = 3, 4, 5, 6, 7, 8$, respectively.

Sequences in Figure 1 are presented in order of an increasing conductance. The color scheme emphasizes general trends: Sequences rich in G:C base pairs are good conductors, while A:T-rich sequences are poor conductors (recall that the Fermi energy is placed at the energy of the G base). Notably, the sequence GCC is not an impressive conductor given that the C bases are placed at the edges. This demonstrates that beyond composition, gateway states allowing for a forceful injection of charge, are crucial for organizing an excellent conductance. Overall, the conductance of 3 bp DNA covers almost 10 orders of magnitude. The best conductor in Fig. 1, CGG, has a non-interrupted path of G-bases, with a single crossing between strands. Next in order are sequences with a single adenine base that carriers

need to traverse. Sequences GGC and CCC are significantly lower in conductance even though they contain only G:C base pairs, since the highest-energy C base is linked to one of the terminals. Finally, sequences with an A:T block are rather poor conductors.

We now include environmental effects, captured by a nonzero probe coupling γ_d . For clarity, Figure 2 depicts the conductance of an $n = 5$ long molecule, but we confirmed that our results are representative for longer chains, $n = 6 - 8$. We organize the sequences in order of increasing conductance at $\gamma_d = 0$, and find roughly three families of rigid molecules: good, poor, and intermediate conductors. Upon turning on the environment, we identify the following trends:

(i) Good conductors with $G = 0.01 - 1 G_0$ are only mildly affected by the environment, see panel a. This indicates that in this case charges proceed through delocalized molecular states. In fact, the conductance here is slightly reduced with the increase of system-bath coupling since scattering processes hamper delocalized motion.

(ii) Poor rigid conductors, sequences 1-100 with $G \lesssim 10^{-10} G_0$, enjoy a dramatic enhancement of their conductance due to the environment. This giant increase over 5-10 orders of magnitude indicates that the underlying transport mechanism has been changed, most likely from off-resonant tunnelling to environmentally-assisted transport. The observed scaling with γ_d further evinces that charge carriers proceed through multi step hopping [37]. A curious observation is that under this mechanism the conductance of sequences 1-100 is almost a constant, see panel c, insensitive to composition and order, which is in a stark contrast to rigid molecules, with sequences 1-100 showing five orders of magnitude variation in conductance.

(iii) Intermediate conductors ($G = 10^{-6} - 10^{-2} G_0$) display significant variability under environmental effects. Sequences that similarly conduct when rigid, greatly digress once environmental effects take place, see panel b. This spreading demonstrates that one should not assume that the quantum coherent (frozen) value represents in any way the behavior of a flexible system. Moreover, these intermediate sequences cannot be categorized as tunneling/ohmic/ballistic conductors. Finally, as we show below, this variability corresponds to clustering of A:T units vs. spreading them apart, which notably only affects the conductance of non-rigid structures.

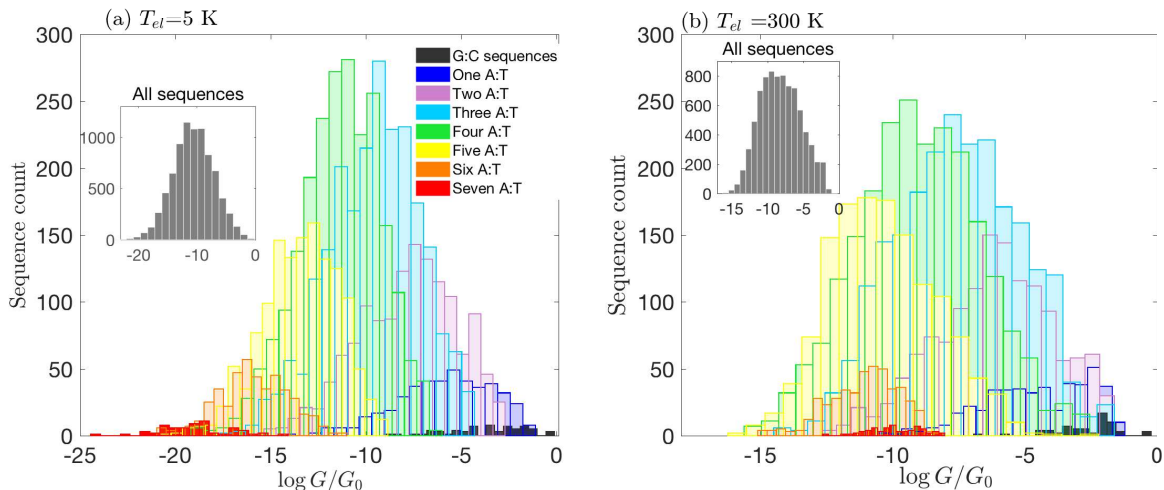


FIG. 3: Conductance histogram for rigid $n = 7$ bp DNA, separated into sequences with different number of A:T base pairs. The inset presents data for all combinations. (a) $T_{el} = 5$ K, (b) $T_{el} = 300$ K. Other parameters are $\gamma_{L,R} = 50$ meV and $\gamma_d = 0$ meV.

C. Composition

Which DNA sequences are poor electrical conductors? Let us first focus on rigid molecules, and watch in Figure 3 the distribution of conductances for an $n = 7$ bp DNA, as well as histograms for different compositions. We find that the rule of thumb, G:C rich sequences being good conductors, is valid. Moreover, at low electronic temperature A:T sequences act as rather poor electrical conductors. One should note however that at room-temperature, sequences with a stacked A segment can support ballistic, band-like current, thus they may conduct more effectively than mixed-nucleotide sequences. Interestingly, the histograms resemble a normal (Gaussian) distribution. The mean of the histogram corresponds to a uniform sequence with an averaged barrier height. The width signifies a strong sensitivity to the arrangement of base pairs within the sequence.

In table II, we exemplify sequences within the three groups: insulators, weak-to-moderate conductors, and excellent conductors. Poor conductors include an A:T block. Having a C base as the edge results in poor conduction. Excellent conductors allow delocalization of charges throughout the sequence. For example, in the CGGGGG sequence, charges enter through the G base, cross to the other strand only once, and continue through the G block un-interrupted until the other metal.

TABLE II: Examples for poor, moderate and excellent $n = 7$ conductors. Conductance is reported for a frozen molecule, $\gamma_d = 0$ at $T_{el} = 5$ K.

Poor, $G < 10^{-11} G_0$	weak-moderate, $10^{-8} < G < 10^{-3} G_0$	good-excellent, $G > 10^{-2} G_0$
ATTTAAA (10^{-21})	ATGGGCA (5×10^{-7})	CCCCGGA (0.010)
AAAAAAA (10^{-20})	CGCATGC (10^{-6})	CACCCGG (0.015)
AATGAAA (10^{-18})	ACGATGG (10^{-6})	CCCCGAG (0.060)
CCTAAAA (10^{-16})	CTCGCGA (10^{-5})	CGGGGGA (0.064)
CAACAAT (10^{-15})	ACGCGGC (10^{-5})	CCGGGGG (0.70)
AAGAATA (10^{-14})	CTCCGTG (10^{-4})	CGGGGGG (0.75)

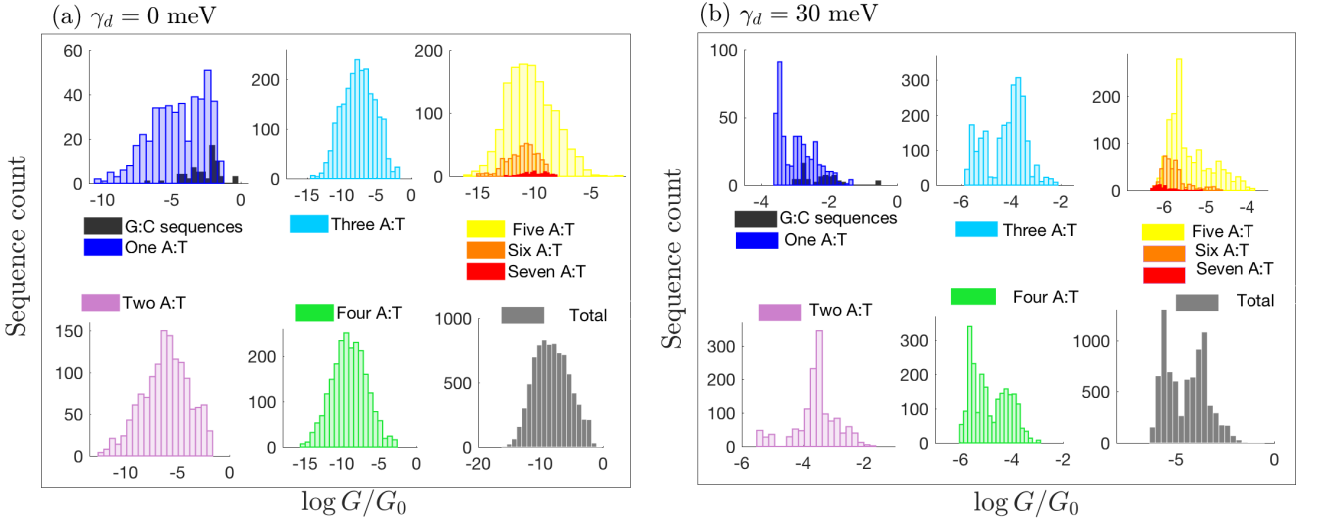


FIG. 4: Histograms of conductance for $n = 7$ bp DNA, divided into groups with different content. (a) $\gamma_d = 0$, (b) $\gamma_d = 30$ meV. Other parameters are $\gamma_{L,R} = 50$ meV and $T_{el} = 300$ K. The insets present conductance histogram for all 8192 sequences.

D. Environmental effects

We turn on the environment in Figure 4, and expose its striking role on the conductance histograms. We find that distributions at finite γ_d not only shift to higher values, compared to the frozen case, but further *split*, showing up as bimodal distributions with a gap in the middle. In Table III we list several sequences that support a comparable electrical conductance when frozen, but receive values 1-2 orders of magnitude apart at finite system-environment interaction. The opening of the gap in the distribution can be rationalized: In rigid structures, the averaged barrier height is a principal variable, as it controls off-resonant conduction. In contrast, once interacting with the environment, carriers can partially localize on the G bases, and hop between them. In this scenario, an A:T segment, such as in AAATCGG, significantly hampers the overall conductance compared to the case with isolated A:T units, as in ACAGTGT, see Table III. The two components in the bimodal distribution therefore correspond to sequences with clustered vs. desolate A:T base pairs. We thus arrive at a critical observation: In rigid structures, the composition essentially determines the conductance, but the structure (base order) is of a lesser importance. In contrast, in flexible molecules transferred charges are highly sensitive to the development of local, enlarged barriers, which disturb site-to-site hopping dynamics.

TABLE III: Role of the structure (clustering) on DNA conductance, $T_{el} = 300$ K, $\gamma_{L,R}=50$ meV

Sequence 5' to 3'	# of A:T bp	$\log G/G_0$ ($\gamma_d = 0$ meV)	$\log G/G_0$ ($\gamma_d = 10$ meV)	$\log G/G_0$ ($\gamma_d = 30$ meV)	A:T block?
AATGCGC	3	-8.0	-6.0	-5.3	yes
ACAGTCG	3	-8.0	-4.1	-3.7	no
AAATCGG	4	-8.0	-6.5	-5.7	yes
ACAGTGT	4	-8.0	-3.8	-3.4	no
AAAAAGG	5	-11.6	-7.0	-6.1	yes
AACAGTA	5	-11.6	-4.3	-4.1	no

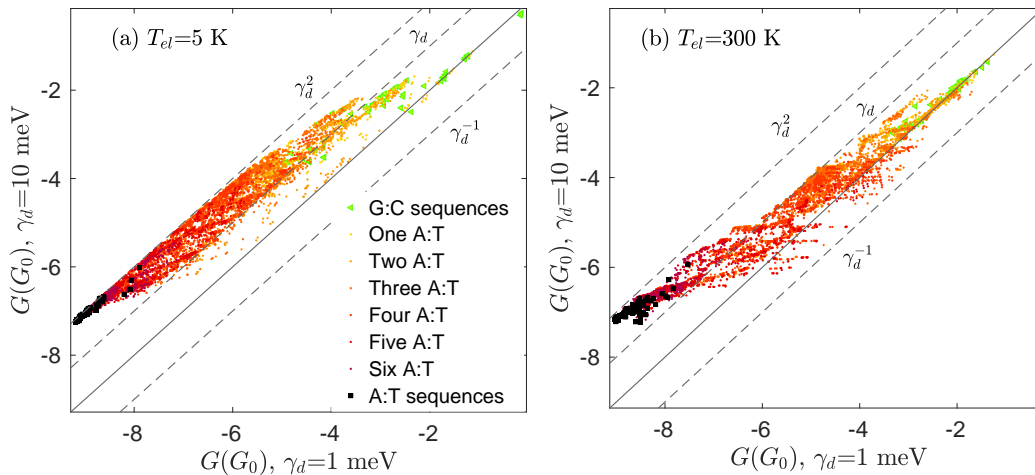


FIG. 5: Effect of environmental fluctuations on the conductance of all $n = 7$ bp DNA molecules, $\gamma_{L,R} = 50$ meV, (a) $T_{el} = 5$ K, (b) $T_{el} = 300$ K. The diagonal (full) identifies sequences that are undisturbed by the environment. The scaling $G \propto \gamma_d^{-1}$, $G \propto \gamma_d$, and $G \propto \gamma_d^2$ are marked by dashed lines.

What is the principal physical mechanism driving charge transfer in dsDNA? In Figure 5 we display the conductances of $n = 7$ bp DNA for two different values of γ_d , 1 meV and 10 meV. Each dot corresponds to a particular sequence, and we make the following observations: (i) The best conductors are found on the diagonal, or below it, meaning, that they are undisturbed or lightly (negatively) affected by incoherent scattering effects. These are in fact stacked G:C molecules that conduct via delocalized states. (ii) The poorest conductors tend to follow the scaling $G \propto \gamma_d^2$. These are mostly A:T sequences with charge transport proceeding via multi-site hopping at finite γ_d . (iii) While we can identify ballistic (green) and ohmic (black) conductors, most molecules display an in-between behavior, $G \propto \gamma_d^\alpha$ with $1 \lesssim \alpha \lesssim 2$ and $0 \lesssim \alpha \lesssim 1$ at low and high electronic temperature, respectively. These sequences conduct via an *intermediate*, coherent-incoherent mechanism, which brings us to one of the principal findings of our work: The majority of 1-5 nanometer long DNA sequences conduct via a mixed quantum-classical mechanism. These molecules cannot be classified as tunneling barriers, ohmic conductors or ballistic wires.

Intermediate conduction mechanisms in DNA, distinct from both deep tunneling and multi-step hopping were revealed in several other studies performed e.g. with the surrogate Hamiltonian approach [24], the phenomenological Buttiker's probe method [25], and the time-dependent stochastic Schrödinger equation [26, 55]. Physically, an intermediate coherent-incoherent behavior results for example from polaron formation involving charge delocalization over several bases [12, 24], or due to the contribution of flickering resonances (achieved through conformational fluctuations) [55].

E. Metal contact: Electronic temperature and hybridization energy

Figure 6 demonstrates the subtle role of the electronic temperature in rigid and flexible molecules. In the former, increasing the electronic temperature dramatically enhances the tunneling conductance, particularly, the conductance of sequences with A:T base pairs. In contrast, scattering of carriers with environmental degrees of freedom results in

their local equilibration at each site, washing out the effect of the incoming charge distribution. A strong response of the conductance to electronic temperature thus indicates on the transition of the transport mechanism, from deep tunneling to resonant transmission, rather than from tunneling to multi-site hopping conduction [37, 41].

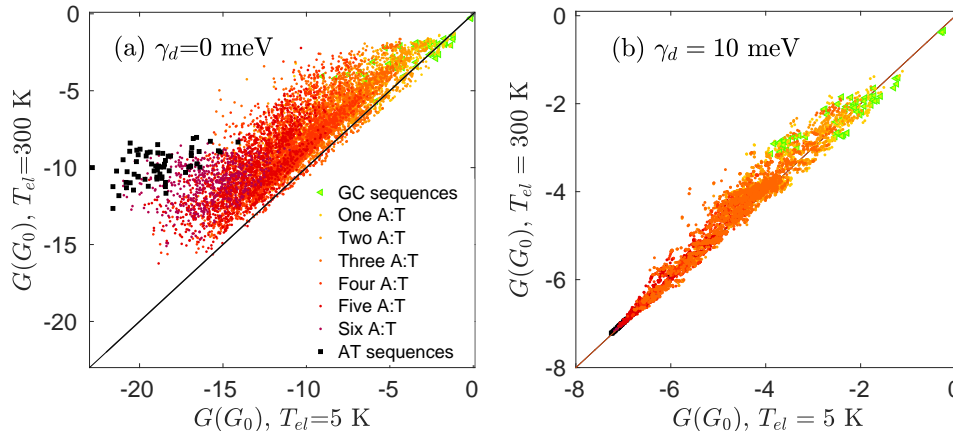


FIG. 6: Effect of the metal temperature T_{el} on the conductance, $n = 7$, $\gamma_{L,R} = 50$ meV, (a) $\gamma_d = 0$, (b) $\gamma_d = 10$ meV.

We argued above that most non-rigid sequences conduct via a mixed, coherent-incoherent mechanism. It is not surprising therefore to find that the metal-molecule hybridization energy influences the conductance of these systems in a rather rich manner, as we show in Figure 7. We find that the electrical conductance scales as $G \propto \gamma_{L,R}^\alpha$ where $-2 \leq \alpha \leq 2$ in rigid structures but $-1 \leq \alpha \leq 1$ at most when $\gamma_d \neq 0$. A:T sequences in particular show a clear adjustment from $\alpha \sim 2$ to $\alpha = 0$ as we turn on the system-environment coupling, indicating on the conversion of transport mechanism from tunneling to multi-site hopping conduction, which is dominated by the bulk of the compound, rather than interface effects.

Figure 7 is involved, and it does not allow us to resolve underlying principles. What are the leading factors influencing the scaling of the conductance with $\gamma_{L,R}$? Figure 8 resolves this question and brings to light the critical role of gateway sites. For simplicity, we focus on a short DNA with 5 bp. We find that if both entry sites are the guanine base, the conductance is almost independent of $\gamma_{L,R}$ in ballistic conductors such as CGGGG. It diminishes with hybridization roughly as $G \propto \gamma_{L,R}^{-2}$ when a barrier is formed, as in CGGAG or CTAAG [67]. In contrast, when the gateway sites are situated far away from the Fermi energy, as in the case of the C and T nucleotides, increasing the broadening enhances the conductance by allowing better injection of carriers into the molecule. Specifically, if both gateway sites are situated off-resonance, as in GAATC, the conductance scales as $G \propto \gamma_{L,R}^2$. In mixed situations, such as having G and T bases at the two boundaries in AGCCG, a nontrivial cancellation effect takes place and $\alpha \sim 0$. Finally, when carriers interact with the environment, the impact of the gateway groups lessens, becoming inconsequential for ohmic conductors. In fact, when $\gamma_d \neq 0$ the metal hybridization mostly affects *intermediate* coherent-incoherent conductors; the poor conductors rely on multi-step hopping, which is rather insensitive to the interface, and the exceptional band-like coherent conductors enjoy a good injection of charge, thus they remain unaffected by the contact energy.

IV. CONCLUSIONS

Fundamental principles in DNA nanoelectronics are distilled here based on direct, all-inclusive simulations. Experiments suggest that electron transfer in 1 – 10 nm-long DNA is highly sensitive to subtle structural variations. Our calculations support this observation. By tuning the effect of the nuclei on charge dynamics we find orders of magnitude enhancement of the electrical conductance, from the deep tunneling coherent limit to the incoherent case. While our calculations obviously suffer from major simplifications that limit the accuracy of calculated values, we bring forward underlying principles for DNA electronics at the nanoscale:

(i) Mostly, natural DNA is a poor electronic material. (ii) The conductance of rigid structures cannot serve as a proxy for the conductance of flexible molecules. In particular, sequences that comparably conduct when frozen may differ by up to 2 orders of magnitude when the molecular environment is allowed to influence the transfer process. (iii) Both the composition (content) and the structure (order) are important in determining the transport behavior of non-rigid molecules. The conductance of sequences rich in G:C nucleotides is generally high compared to those containing predominantly A:T nucleotides. DNA sequences with an island of A:T units show a lower conductance

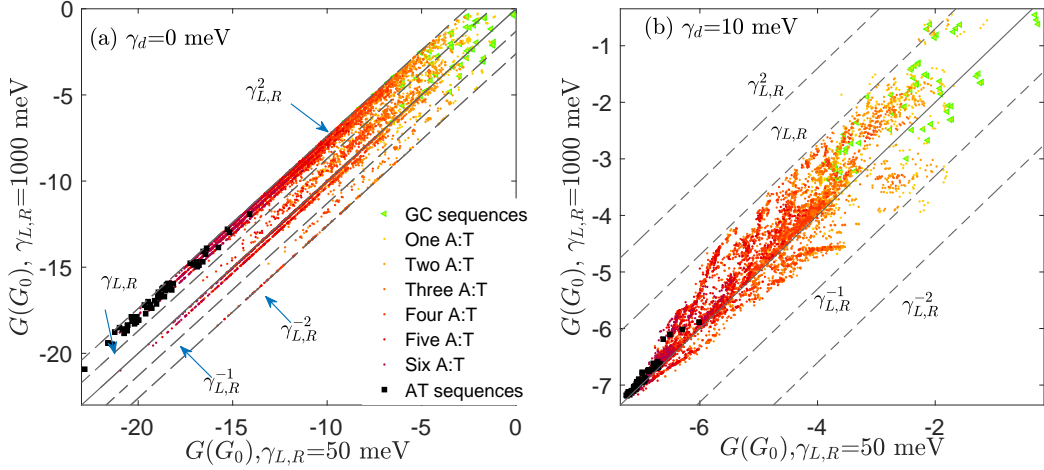


FIG. 7: Effect of the metal-molecule coupling $\gamma_{L,R}$ on the conductance of $n = 7$ bp DNA molecules, $T_{el} = 5$ K. (a) $\gamma_d = 0$ meV, (b) $\gamma_d = 10$ meV. The different scalings are marked by dashed lines.

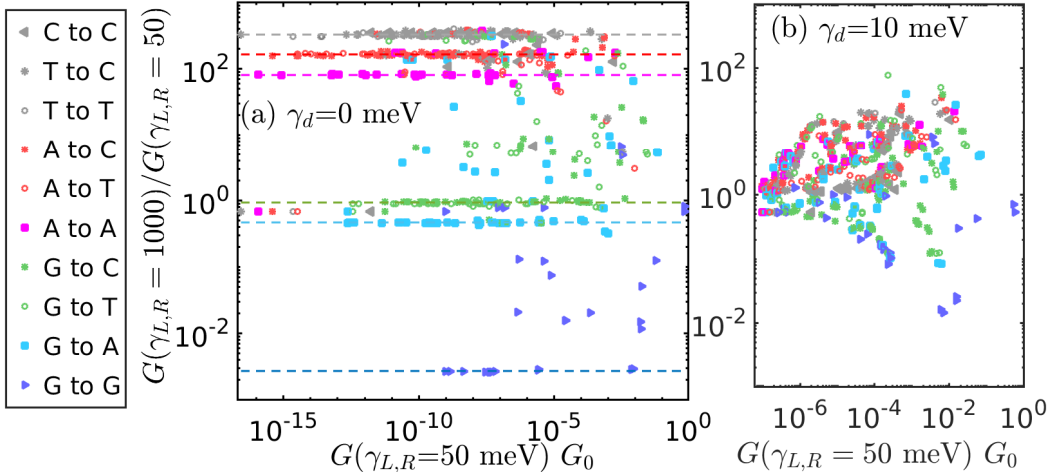


FIG. 8: Ratio of conductances at different values of $\gamma_{L,R}$ for an $n = 5$ dsDNA. Symbols correspond to different families of sequences, prepared based on the identity of the entry bases. For example, gray triangles mark molecules with C bases at the boundaries, the gray * symbol indicates on molecules with T and C bases at the edges, $T_{el} = 5$ K, (a) $\gamma_d = 0$ meV, (b) $\gamma_d = 10$ meV. Dashed lines highlight the scaling behavior of selected classes of molecules.

compared to sequences in which A:T base pairs are placed apart from each other. (iv) Gateway states largely affect the conductance of rigid molecules. Moreover, the role of the metal-molecule contact is influential in many intermediate coherent-incoherent conductors. (v) Lastly, the majority of DNA molecules examined here conduct via a mixed quantum-classical (coherent-incoherent) mechanism. Only few, special sequences can be classified as tunneling barriers, ohmic conductors, or ballistic molecular wires. Our main finding is that quantum coherent effects are prevalent, and they play a central role in biological electron transport over the distance of few nanometers. It is interesting to explore similar questions of electron transfer through proteins [71].

In closing this computational search, which sequences come forward as good and robust conductors? Not surprisingly, we find that conjugated G:C sequences with a *single* crossing between strands are superb conductors with $G \sim 0.3 - 0.75 G_0$ across a wide range of parameters; recall that the electrodes are connected to the 3' ends. The crossing between strands should minimally disturb the π conjugation, thus the best e.g. $n = 7$ sequence is CGGGGGG, while the next best sequences are CCGGGGG and CCCGGGG, and so on. These molecules are only lightly affected by the metal-molecule contact and the coupling to the surrounding environment. Other good and relatively robust, though less obvious sequences are those with an adenine at one end, a segment of unperturbed G bases, and a single crossing between strands, for example, CGGGGGA and TCGGGGG, coming up with $G \sim 0.1 G_0$. These

molecules are robust against the nuclear environment, and strengthening the metal-molecule contact enhances their conductance. According to our calculations, the best DNA electrical conductors support charge transport through delocalized states. This band-like coherent motion is robust against environmental interactions. Nevertheless, it is important to remember that e.g., out of the 8192 different sequences with $n = 7$ base-pairs, we identify here only very few (~ 5) excellent and robust conductors.

Our computational method suffers from several obvious shortcomings: The electronic Hamiltonian is included at a coarse grained level, with each base represented by a single electronic site using a fixed parametrization. A realistic molecule-electrode coupling model is missing in our treatment, and we capture this coupling with a single parameter. Furthermore, in all calculations we place the Fermi energy of the electrodes at the energy of the guanine base. The electronic structure could be improved by treating the contact atoms explicitly, and by generating an electronic Hamiltonian for each sequence separately. Another weakness of our framework is that the dynamics of the environment is not explicitly treated. We encapsulate scattering effects of conducting charge carriers from different sources (low and high frequency phonon modes, polarization effects, static and dynamical fluctuations) into a single, constant parameter that dictates decoherence and energy relaxation. One could improve our method from here by e.g. providing distinct scattering lifetimes on different sites, and by averaging over a static disorder. Overall, state of the art QM/MD simulations are costly and impractical for our purposes, while the low-level Landauer-Büttiker framework employed here provides a meaningful starting point for performing large scale simulations beyond the coherent quantum limit.

Our minimal treatment of DNA nanoelectronics is not expected to be in quantitative agreement with experiments, but it is powerful enough to uncover fundamental principles, most importantly, that the majority of inspected molecules display mixed coherent-incoherent charge transport characteristics. We aspire this work to stimulate experimental tests as well as more precise calculations that could guide the search for DNA molecules with desired electronic properties. Finally, chiral-induced spin selectivity through double helical DNA critically depends on the nucleobase fluctuations [72, 73]. The present framework can be readily extended to explore spin-polarized charge current effects [74].

Acknowledgments

DS acknowledges support from an NSERC Discovery Grant and the Canada Research Chair program. The work of RK was supported by the CQIQC summer fellowship at the University of Toronto and the University of Toronto Excellence Research Fund.

-
- [1] T. Chakraborty, *Charge Migration in DNA; Perspectives from Physics, Chemistry, and Biology*, (Springer-Verlag: Berlin, 2007).
 - [2] J. C. Genereux and J. K. Barton, Mechanisms for DNA Charge Transport, *Chemical Reviews* **110**, 1642-1662 (2010).
 - [3] A. R. Arnold, M. A. Grodick, and J. K. Barton, DNA Charge Transport: From Chemical Principles to the Cell, *Cell Chemical Biology* **23**, 183 (2016).
 - [4] D. Yang, M. R. Hartman, T. L. Derrien, S. Hamada, D. An, K. G. Yancey, R. Cheng, M. Ma, and D. Luo, DNA Materials: Bridging Nanotechnology and Biotechnology, *Acc. Chem. Res.* **47**, 1902-1911 (2014).
 - [5] E. Stulz (Editor), G. H. Clever (Editor), *DNA in Supramolecular Chemistry and Nanotechnology*, Wiley (2015).
 - [6] Y. Zhang, W. B. Zhang, C. Liu, P. Zhang, A. Balaeff, and D. N. Beratan, DNA charge transport: Moving beyond 1D, *Surf. Sci.* **652**, 33-38 (2016).
 - [7] D. N. Beratan, R. Naaman, and D. H. Waldeck, Charge and Spin Transport Through Nucleic Acids, <https://doi.org/10.1016/j.coelec.2017.08.017>
 - [8] D. Porath, N. Lapidot, and J. Gomez-Herrero, Charge Transport in DNA-Based Devices, in *Introducing Molecular Electronics*, Lect. Notes Phys. 680 (Springer-Verlag, Berlin Heidelberg 2005) Eds. G. Cuniberti, G. Fagas, and K. Richter, 411-444.
 - [9] B. Xu, P. Zhang, X. Li, and N. Tao, Direct Conductance Measurements of Single DNA Molecules in Aqueous Solution, *Nano Lett.* **4**, 1105-1108 (2004).
 - [10] D. Dulic, S. Tuukkanen, C.-L. Chung, A. Isambert, P. Lavie, and A. Filoramo, Direct Conductance Measurements of Short Single DNA Molecules in Dry Conditions, *Nanotechnology* **20**, 115502 (2009).
 - [11] F. D. Lewis, H. Zhu, P. Daublain, T. Fiebig, M. Raytchev, Q. Wang, and V. Shafirovich, Crossover From Superexchange to Hopping as the Mechanism for Photoinduced Charge Transfer in DNA Hairpin Conjugates. *J. Am. Chem. Soc.* **128**, 791-800 (2006).

- [12] M. A. Harris, A. K. Mishra, R. M. Young, K. E. Brown, M. R. Wasielewski, and F. D. Lewis, Direct Observation of the Hole Carriers in DNA Photoinduced Charge Transport, *J. Am. Chem. Soc.* **138**, (17), 5491-5494 (2016).
- [13] S. O. Kelley and J. K. Barton, Electron Transfer Between Bases in Double Helical DNA, *Science* **283**, 375 (1999).
- [14] B. Giese, J. Amaudrut, A.-K. Köhler, M. Spormann, and S. Wessely, Direct Observation of Hole Transfer Through DNA by Hopping Between Adenine Bases and by Tunnelling, *Nature* **412**, 318-320 (2001).
- [15] C. H. Wohlgamuth, M. A. McWilliams, and J. D. Slinker, DNA as a Molecular Wire: Distance and Sequence Dependence, *Anal. Chem.* **85**, 8634-8640 (2013).
- [16] Y. Li, L. Xiang, J. Palma, Y. Asai, and N. Tao, Thermoelectric Effect and its Dependence on Molecular Length and Sequence in Single DNA Molecules, *Nature Comm.* **7**, 11294 (2016).
- [17] E. Beall, S. Ulku, C. Liu, E. Wierzbinski, Y. Zhang, Y. Bae, P. Zhang, C. Achim, D. N. Beratan, and D. H. Waldeck, Effects of the Backbone and Chemical Linker on the Molecular Conductance of Nucleic Acid Duplexes, *J. Am. Chem. Soc.* **139**, 6726-6735 (2017).
- [18] S. Xuan, Z. Meng, X. Wu, J.-R. Wong, G. Devi, E. K. L. Yeow, and F. Shao, Efficient DNA-Mediated Electron Transport in Ionic Liquids, *ACS Sustainable Chemistry and Engineering* **4**, 6703-6711 (2016).
- [19] J. M. Artes, Y. Li, J. Qi, M.P. Anantram, and J. Hihath, Conformational Gating of DNA Conductance, *Nature Comm.* **6**, 8870 (2015).
- [20] N. Renaud, M. A. Harris MA , A. P. N. Singh, Y. A. Berlin, M. A. Ratner, M. R. Wasielewski ,F. D. Lewis, F. C. Grozema: Deep-Hole Transfer Leads to Ultrafast Charge Migration in DNA Hairpins, *Nat. Chem.* **8** 1015-1021 (2016).
- [21] K. L. Jimenez-Monroy, N. Renaud, J. Drijkoningen, D. Cortens, K. Schouteden, C. van Haesendonck, W. J. Guedens, J. V. Manca, L. D. A. Siebbeles, F. C. Grozema, and P. H. Wagner, High Electronic Conductance through Double-Helix DNA Molecules with Fullerene Anchoring Groups, *J. Phys. Chem. A* **121**, 1182-1188 (2017).
- [22] L. Xiang, J. L. Palma, Y. Li, V. Mujica, M. A. Ratner, and N. Tao, Gate-Controlled Conductance Switching in DNA, *Nature Comm.* **8**, 14471 (2017).
- [23] J. D. Slinker, N. B. Muren, S. E. Renfrew, and J. K. Barton, DNA Charge Transport Over 34 nm, *Nat. Chem.* **3**, 228-233 (2011).
- [24] N. Renaud, Y. A Berlin, F. D. Lewis, and M. A. Ratner, Between Superexchange and Hopping: An Intermediate Charge-Transfer Mechanism in Poly(A)-Poly(T) DNA Hairpins, *J. Am. Chem. Soc.* **135**, 3953-3963 (2013).
- [25] L. Xiang, J. L. Palma, C. Bruot, V. Mujica, M. A. Ratner, and N. Tao, Intermediate Tunneling-Hopping Regime in DNA Charge Transport, *Nat. Chem.* **7**, 221-226 (2015).
- [26] C. Liu, L. Xiang, Y. Zhang, P. Zhang, D. N. Beratan, Y. Li, and N. Tao, Engineering Nanometer-Scale Coherence in soft Matter, *Nat. Chem.* **8**, 941-945 (2016).
- [27] M. Büttiker, Small Normal-Metal Loop Coupled to an Electron Reservoir, *Phys. Rev. B* **32**, 1846 (1985).
- [28] M. Büttiker, Role of Quantum Coherence in Series Resistors, *Phys. Rev. B* **33**, 3020 (1986).
- [29] J. L. DAmato and H. M. Pastawski, Conductance of a Disordered Linear Chain Including Inelastic Scattering Events, *Phys. Rev. B* **41**, 7411 (1990).
- [30] H. M. Pastawski, Classical and Quantum Transport from Generalized Landauer-Büttiker Equations. II. Time-Dependent Resonant Tunneling, *Phys. Rev. B* **46**, 4053 (1992).
- [31] D. Roy and A. Dhar, Electron Transport in a One Dimensional Conductor with Inelastic Scattering by Self-Consistent Reservoirs, *Phys. Rev. B* **75**, 195110 (2007).
- [32] D. Nozaki, Y. Girard, and K. Yoshizawa, Theoretical Study of Long-Ranged Electron Transport in Molecular Junctions, *J. Phys. Chem. C* **112**, 17408 (2008).
- [33] D. Nozaki, C. Gomes da Rocha, H. M. Pastawski, and G. Cuniberti, Disorder and Dephasing Effects on Electron Transport through Conjugated Molecular Wires in Molecular Junctions, *Phys. Rev. B* **85**, 155327 (2012).
- [34] J. Qi, N. Edirisinghe, M. G. Rabbani, and M. Anantram, Unified Model for Conductance Through DNA with the Landauer-Büttiker Formalism, *Phys. Rev. B*, **87** 085404 (2013).
- [35] S. G. Chen, Y. Zhang, S. K. Koo, H. Tian, C. Y. Yam, G. H. Chen, and M. A. Ratner, Interference and Molecular Transport-A Dynamical View: Time-Dependent Analysis of Disubstituted Benzenes, *J. Phys. Chem. Lett.* **5**, 2748 (2014).
- [36] R. Venkataramani, E. Wierzbinski, D. H. Waldeck, and D. N. Beratan, Breaking the Simple Proportionality Between Molecular Conductances and Charge Transfer Rates, *Faraday Discuss.* **174**, 57 (2014).
- [37] M. Kilgour and D. Segal, Charge Transport in Molecular Junctions: From Tunneling to Hopping With the Probe Technique, *J. Chem. Phys.* **143**, 024111 (2015).
- [38] M. Kilgour and D. Segal, Tunneling Diodes Under Environmental Effects, *J. Phys. Chem. C* **119**, 25291-25297 (2015).
- [39] M. Kilgour and D. Segal, Inelastic Effects in Molecular Transport Junctions: The Probe Technique at High Bias, *J. Chem. Phys.* **144**, 124107 (2016).
- [40] R. Korol, M. Kilgour, D. Segal, Thermopower in Molecular Junctions: Tunneling to Hopping Crossover in DNA, *J. Chem. Phys.* **145**, 224702 (2016).
- [41] H. Kim and D. Segal, Controlling Charge Transport Mechanisms in Molecular Junctions: Distilling Thermally-Induced Hopping from Coherent-Resonant Conduction, *J. Chem. Phys.* **146**, 164702 (2017).
- [42] R. Korol, M. Kilgour, and D. Segal, *Comp. Phys. Comm.* (2017).
- [43] H. Kim, M. Kilgour, and D. Segal, Intermediate Coherent-Incoherent Charge Transport: DNA as a Case Study, *J. Phys. Chem. C* **120**, 23951-23962 (2016).
- [44] R. Gutierrez, S. Mohapatra, H. Cohen, D. Porath, and G. Cuniberti, Inelastic Quantum Transport in a Ladder Model: Implications for DNA Conduction and Comparison to Experiments on Suspended DNA Oligomers, *Phys. Rev. B* **74**, 235105 (2006).

- [45] N. V. Grib, D. A. Rydnyk, R. Guitierrez, and G. Cuniberti, Distance Dependent Coherent Charge transport in DNA: Crossover from Tunneling to Free Propagation, *J. Biophys. Chem.* **1**, 77-85 (2010).
- [46] J. Yi, Conduction of DNA Molecules: A Charge-Ladder Model, *Phys. Rev. B* **68**, 193103 (2003).
- [47] D. Klotsa, R. A. Roemer, and M. S. Turner, Electronic Transport in DNA, *Biophys. J.* **89**, 2187 (2005).
- [48] X. F. Wang and T. Chakraborty, Charge Transfer via a Two-Strand Superexchange Bridge in DNA, *Phys. Rev. Lett.* **97**, 106602 (2006).
- [49] K. Senthilkumar, F. C. Grozema, C. F. Guerra, F. M. Bickelhaupt, F. D. Lewis, Y. A. Berlin, M. A. Ratner, and L. D. A. Siebbeles, Absolute Rates of Hole Transfer in DNA, *J. Am. Chem. Soc.* **127**, 14894-14903 (2005).
- [50] M. Zilly, O Ujsaghy, and D. E. Wolf, Conductance of DNA Molecules: Effects of Decoherence and Bonding, *Phys. Rev. B* **82**, 125125 (2010).
- [51] T. Tsukamoto, Y. Ishikawa, Y. Sengoku, and N. Kurita, *Chem. Phys. Lett.* **474**, 362 (2009)
- [52] D. Reha, A. A. Voityuk, and S. A. Harris, An in Silico Design for a DNA Nanomechanical Switch, *ACS Nano* **4**, 5737 (2010).
- [53] A. Staykov, Y. Tsuji, and K. Yoshizawa, Conductance Through Short DNA Molecules, *J. Phys. Chem. C* **115**, 3482 (2011).
- [54] In the parametrization of Ref. [49], on-site energies depend on the identity of neighboring bases. This variation of energy from site to site, even in a uniform chain, largely destroys coherent resonant dynamics, which can be recovered by the occurrences of “flickering resonances”, achieved through conformational fluctuations [55]. Here, we simplify this description and assign a single, averaged value for on-site energies for each base, see Table I. As we argue in Ref. [40], the combined effect of site energy variations with flickering resonances is practically comparable to a model with fixed site energies suffering level broadening γ_d . We also performed simulations directly with the parameter set of Ref. [49], without averaging over site energies. These results are very similar to those reported in the main body of the paper, only missing the coherent-molecular wire component—which should be revived by structural fluctuations.
- [55] Y. Zhang, C. Liu, A. Balaeff, S. S. Skourtis, and D. N. Beratan, Biological Charge Transfer via Flickering Resonance, *Proc. Natl. Acad. Sci. U.S.A* **111**, 10049-10054 (2014).
- [56] C. Liu, D. N. Beratan, and P. Zhang, Coarse-Grained Theory of Biological Charge Transfer with Spatially and Temporally Correlated Noise, *J. Phys. Chem. B* **120**, 3624-3633 (2016).
- [57] P. Woiczikowski, T. Kubar, R. Gutierrez, R. Caetano, G. Cuniberti, and M. Elstner, Combined DFT and Landauer Approach for Hole Transfer in DNA Along Classical MD Trajectories, *J. Chem. Phys.* **130**, 215104 (2009).
- [58] M. H. Lee, S. Avdoshenko, R. Gutierrez, and G. Cuniberti, Charge Migration Through DNA Molecules in the Presence of Mismatches, *Phys. Rev. B* **82**, 155455 (2010).
- [59] R. Gutierrez, R. Caetano, P. B. Woiczikowski, T. Kubar, M. Elstner, and G. Cuniberti, Structural Fluctuations and Quantum Transport through DNA Molecular Wires: a Combined Molecular Dynamics and Model Hamiltonian Approach, *New J. Phys.* **12**, 023022 (2010).
- [60] T. Kubar, U. Kleinekathöfer, and M. Elstner, Solvent Fluctuations Drive the Hole Transfer in DNA: A Mixed Quantum-Classical Study, *J. Phys. Chem. B* **113**, 13107-13117 (2009).
- [61] T. Kubar, M. Elstner, B. Popescu, and U. Kleinekathöfer, Polaron Effects on Charge Transport through Molecular Wires: A Multiscale Approach, *J. Chem. Theory and Comp.* **13**, 286-296 (2017).
- [62] M. Wolter, M. Elstner, U. Kleinekathöfer, and T. Kubar, Microsecond Simulation of Electron Transfer in DNA: Bottom-Up Parametrization of an Efficient Electron Transfer Model Based on Atomistic Details, *J. Phys. Chem. B* **121**, 529-549 (2017).
- [63] D. Brisker-Klaiman and U. Peskin, Ballistic Charge Transport through Bio-Molecules in Dissipative Environment, *Phys. Chem. Chem. Phys.* **14**, 13835-13840 (2012).
- [64] F. Grozema, Y. A. Berlin, and L. D. A. Siebbeles, Mechanism of Charge Migration through DNA: Molecular Wire Behavior, Single-Step Tunneling or Hopping? *J. Am. Chem. Soc.* **122**, 10903-10909 (2000).
- [65] G. Benenti, G. Casati, K. Saito, and R. S. Whitney, Fundamental Aspects of Steady-State Conversion of Heat to Work at the Nanoscale, *Phys. Rep.* **694**, 1 (2017)
- [66] S. Bedkihal, M. Bandyopadhyay, and D. Segal, The Probe Technique Far-From-Equilibrium: Magnetic Field Symmetries of Nonlinear Transport, *Euro. Phys. J. B* **86**, 506 (2013).
- [67] A. Nitzan, *Chemical Dynamics in Condensed Phases: Relaxation, Transfer, and Reactions in Condensed Molecular Systems*, (Oxford University Press, Oxford, 2006).
- [68] M. Di Ventra, *Electrical Transport in Nanoscale Systems*, (Cambridge University Press, Cambridge, U.K., 2008).
- [69] The matrices are given by $(\hat{\Gamma}_{i \neq 1, N})_{p, q} = \gamma_d \delta_{p, i} \delta_{q, i}$, $(\hat{\Gamma}_1)_{p, q} = (\gamma_d + \gamma_L) \delta_{p, 1} \delta_{q, 1}$, and $(\hat{\Gamma}_N)_{p, q} = (\gamma_d + \gamma_R) \delta_{p, N} \delta_{q, N}$ with the $i = 1$ site coupled to the left metal, and site $N = 2n$ coupled to the right lead.
- [70] A. A. Voityuk, K. Siriwong, and Notker Rösch, Environmental Fluctuations Facilitate Electron- Hole Transfer from Guanine to Adenine in DNA π Stacks, *Angew. Chem. Int. Ed.* **43**, 624-627 (2004).
- [71] M. P. Ruiz, A. C. Aragones, N. Camarero, J. G. Vilhena, M. Ortega, L. A. Zotti, R. Perez, J. Carlos Cuevas, P. Gorostiza, and I. Diez-Perez, Bioengineering a Single-Protein Junction, *J. Am. Chem. Soc.* **139**, 15337-15346 (2017).
- [72] B. Goehler, V. Hamelbeck, T.Z. Markus, M. Kettner, G.F. Hanne, Z. Veger, R. Naaman, and H. Zacharias, Spin Selectivity in Electron Transmission Through Self-Assembled Monolayers of Double-Stranded DNA, *Science* **331**, 894-897 (2011).
- [73] D. N. Beratan, R. Naaman, and D. H. Waldeck, Charge and Spin Transport Through Nucleic Acids, *Current Opinion in Electrochemistry* (2017). <https://doi.org/10.1016/j.coelec.2017.08.017>
- [74] A.-M. Guo and Q.-f. Sun, Spin-Selective Transport of Electrons in DNA Double Helix, *Phys. Rev. Lett.* **108**, 218102 (2012).